Indian Journal of Engineering & Materials Sciences
Vol. 33, April 2026, pp. 176-183
DOI: 10.56042/ijems.v33i02.23314

Structural analysis and classification of silver–graphene oxide (Ag-GO) nanocomposites using SAM-based segmentation and machine learning models

Parashuram Bannigidad[a], Sagar Chingali[a*] & Prabhuodeyara Gurubasavaraj[b]

[a]Department of Computer Science, Rani Channamma University, Belagavi 591 156, Karnataka

[b]Department of Chemistry, Rani Channamma University, Belagavi 591 156, Karnataka

Received: 01 September 2025; accepted: 14 January 2026

Nanocomposites have acquired significant interest in antimicrobial, catalytic, and electronic applications due to their synergistic properties. The morphology and structural arrangements of nanocomposites at the micro and nanoscale have been recognized as strong determinants of these functional properties. This study has addressed the Structural Activity Relationship (SAR) of Silver–Graphene Oxide (Ag–GO) nanocomposites by employing a methodology to segment and classify the nanocomposites. Scanning Electron Microscopy (SEM) images have been used to segment nanocomposites using the Segment Anything Model (SAM) and to extract structural features such as area, perimeter, aspect ratio, eccentricity, and circularity, enabling the classification of nanocomposites using various machine learning models. Supervised machine learning techniques, namely Random Forest, Logistic Regression, Decision Tree, K-Nearest Neighbours (KNN) and XGBoost, have been employed for nanocomposite classification. This study has addressed a critical gap by incorporating automated segmentation and robust classification within a transparent performance evaluation framework, where XGBoost has demonstrated the highest classification accuracy of 97% for shape and 95% for size, outperforming other models in identifying and categorizing diverse morphological patterns within Ag–GO nanocomposites.

Keywords: Classification, Machine learning, Metal oxide nanocomposites, Morphology, SAM, Silver–Graphene oxide, Structural activity relationship, XGBoost

1 Introduction

Nanocomposites have acquired significant interest in antimicrobial, catalytic, and electronic work due to their synergistic properties. The morphology and structural arrangements of nanocomposites at the micro- and nanoscale have also been strong determinants of these functional properties. SEM image interpretation, however, has been subjective and cumbersome. Recent advances in computer vision, particularly the segment anything model (SAM), have become an effective tool for automated and precise nanostructure segmentation. This study has been devoted to the application of SAM to facilitate high-resolution segmentation of Ag–GO nanocomposites in SEM images and to employ machine learning approaches to identify important structure–activity relationships. Nanostructures have been categorized, and their distribution patterns within the composite matrix have been plotted by quantifying features related to shape, size, and texture. Green nanomaterials have been produced using alternative approaches rather than traditional chemical methods. Green strategies have aimed to reduce the use of toxic reagents while maintaining functional integrity. Kahraman[1] has prepared silver-doped graphene oxide nanocomposites through green synthesis and has demonstrated promising electrochemical behaviour. Nam[2] has prepared silver–graphene oxide nanocomposites using plant extracts, showing potential antibacterial and sensing capabilities. Ag/GO nanocomposites have been effectively applied in biomedical treatment and environmental remediation as reported by Thinh[3] and Malik[4]. Ag-GNP nanocomposites exhibit enhanced antimicrobial and photocatalytic activities Jamjoum[5] and Kumari[6]. Gurubasavaraj[7] has demonstrated that nanocomposites synthesized through microwave-assisted green methods exhibit high antioxidant and antibacterial characteristics. Li[8] has reported antifungal behaviour demonstrating synergistic effects between graphene oxide and silver. Das[9] has developed a green-synthesized reduced graphene oxide–silver nanoparticle catalyst capable of degrading a broad range of organic pollutants. Ji[10] and Yang[11] have applied machine learning approaches to model nanomaterial structure–property relationships, enabling accurate prediction.

*Corresponding author (E-mail:sagar.chingali@gmail.com

The development of electron microscopy has emphasized the need for accurate segmentation of nanocomposites. The Segment Anything Model has been successfully integrated into nanocomposite imaging, enabling efficient detection and labelling. Abebe[12] has applied SAM for automated nanocomposite segmentation and feature extraction in electron microscopy. Monteiro[13] and Gaines[14] have demonstrated that SAM and AI vision models significantly reduce manual workload while ensuring accurate morphological quantification. Lu[15] has shown that machine learning enables automated morphological classification and accurate segmentation in TEM images, providing a foundation for domain size quantification and shape analysis. Papia[16] has demonstrated that machine learning techniques enable automated and accurate SEM image analysis, including pore size distribution, shape classification, and image enhancement. Bannigidad[17] has applied machine learning models to segment and classify metal and metal oxide nanoparticles in SEM and TEM images. Jahanian[18] has shown that machine learning-based models reliably extract and classify nanomaterial structural features from microscopy images. Xu[19] and Prasad[20] have proposed predictive models to assess silver nanocomposite morphology and size, enhancing quality control. Tao[21] and Saxena[22] have emphasized the role of machine learning in optimizing synthesis conditions and predicting physicochemical properties of nanocomposites, thereby reducing trial-and-error experimentation. Zhong[23] has demonstrated the integration of pre-trained models such as SAM with custom image analysis pipelines for automated segmentation and particle size quantification. Shah[24] has introduced neural-network-based segmentation to overcome the labour-intensive and subjective nature of conventional SEM image analysis.

Understanding structure–activity relationships has enabled targeted nanocomposite design. Araujo[25] has demonstrated the effectiveness of metal oxide nanocomposites for photocatalytic remediation of organic water contaminants. Xie[26] and Lange[27] have reviewed antibacterial mechanisms of nanomaterials, linking surface charge, size, and functional groups to antimicrobial efficacy. Singh[28] has explored the influence of silver-functionalized graphene oxide on thermo-physical and optical properties, contributing to thermal management applications. Yu[29] has reviewed graphene oxide-based sensors and highlighted structure–activity relationship-driven improvements in strain sensitivity. Bannigidad[30] has proposed an automated machine learning model for silver nanoparticles SEM analysis and classification, addressing the limitations of conventional methods. Negi[31] has primarily relied on conventional biological and chemical evaluation methods without exploring machine learning models for predicting biological activity or classifying nanostructures using imaging data. Although extensive research has been conducted on the green synthesis and characterization of nanocomposites, significant gaps have remained in the application of automated and data-driven techniques. Previous studies have lacked automated segmentation, limiting reproducibility and scalability. Quantitative structure–activity frameworks based on image-derived features and machine learning classification outcomes have not been incorporated. Additionally, several studies have applied statistical tools without benchmarking performance using standard evaluation metrics such as confusion matrices and ROC–AUC curves. No integrated pipeline combining general-purpose segmentation via SAM with multiple machine learning classifiers including Random Forest, Logistic Regression, KNN, Decision Tree, and XGBoost has been developed for nanocomposite evaluation. Therefore, this study has addressed a critical gap by integrating automated segmentation with robust classification and transparent performance evaluation to identify and categorize morphological patterns in Ag–GO nanocomposites, facilitating effective mapping of nanostructure morphology to functional properties.

2 Materials and Methods

Synthesis and characterization of Ag-GO nanocomposites was carried out in the laboratory of Dr. P. M. Gurubasavaraj in the Department of Chemistry at Rani Channamma University, Belagavi. The synthesis and characterization of Ag-GO nanocomposites are as below.

2.1 Biogenic synthesis of silver oxide (Ag_2O) nanoparticles

Silver oxide (Ag_2O) nanoparticles were produced in a biogenic way. In a double necked R B flask, silver nanoparticles solution was taken and 0.2 M NaOH was added dropwise while maintaining a basic pH of 8–9. Using a thermocouple, the mixture temperature was kept at 80° C and refluxed for 2 hours. The precipitate obtained was evaporated in a hot air oven at 10^{o} C to collect it in a petri dish. Dried particles were then calcined in a muffle furnace at 600^{o} C during 3 hours to attain Ag_2O nanoparticles.

2.2 Synthesis of Ag–GO nanocomposites

To prepare Ag-GO nanocomposites, 0.5 g of silver (Ag) nanoparticles and 0.25 g of graphene oxide (GO) were weighed accurately and mixed thoroughly following 5-6 hours in agate mortar and grinded well to form Ag-GO nanocomposites.

2.3 Characterization

SEM coupled with EDX was used to examine the morphological characteristics of the synthesized Ag-GO nanocomposites. A JSM-7100F JEOL microscope was used to obtain SEM images with 250x to 25000x magnifications. These methods were used to verify the morphology, structure, and composition of elements of the synthesized nanocomposites at the surface level.

2.4 Proposed method

In this work, we have used SAM model to segment nanocomposites and several machine learning classification models to analyze Silver-Graphene Oxide (Ag-GO) nanocomposites using Scanning Electron Microscopy (SEM) images. The initial step involved capturing high-resolution SEM images of Ag–GO nanocomposites. Next, the grayscale images were pre-processed using CLAHE for enhancing the contrast. For, compatibility with the input format of the Segment Anything Model (SAM), images were subsequently converted to RGB. The pre-trained SAM model (ViT-H variant) was employed to segment individual nanocomposites using mask generation. Post-processing steps were applied to refine mask boundaries and eliminate noise. A composite mask and corresponding colour overlay were generated to visually confirm segmentation accuracy. Fig. 1 represents the flow diagram of the proposed methodology.

Following segmentation, we extracted both geometric features from each identified nanocomposite.

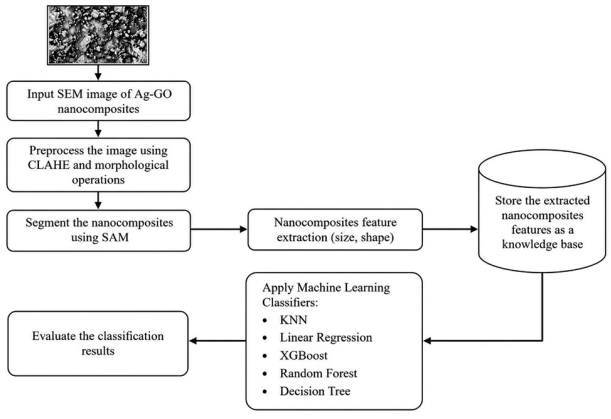

Fig. 1 —Flow diagram of the proposed methodology.

Geometric features included area, perimeter, equivalent diameter, aspect ratio, eccentricity, and circularity. A feature matrix was created, and nanocomposites were annotated with shape and size labels. We divided the dataset into two subsets: 80% for training the models and 20% for testing. Five supervised machine learning models were trained and evaluated for classification purposes: Random Forest, Logistic Regression, Decision Tree, K-Nearest Neighbors (KNN), and XGBoost. Performance was evaluated using metrics such as accuracy, precision, recall, F1-score, confusion matrix and ROC curve. Step by step procedure of the proposed methodology is as shown in the following algorithm.

Algorithm for Ag-GO nanocomposites segmentation and classification:

Step 1 : Load the Silver Graphene Oxide (Ag-GO) SEM image and convert it to grayscale image.
Step 2 : Apply CLAHE to grayscale image to enhance contrast.
Step 3 : Convert grayscale image to RGB format for compatibility with SAM input.
Step 4 : Load the SAM model with specific mask generator parameters.
Step 5 : Generate segmentation masks for individual nanocomposites using SAM.
Step 6 : Label segmented nanocomposites and extract features: Area, perimeter, aspect ratio, eccentricity, circularity.
Step 7 : Construct a feature matrix and assign shape and size class labels to each nanocomposite.
Step 8 : Divide the dataset into training (80%) and testing (20%) for model evaluation.
Step 9 : Train machine learning models: Random Forest, Logistic Regression, Decision Tree, KNN, XGBoost for shape and size classification.
Step 10 : Test machine learning models: Random Forest, Logistic Regression, Decision Tree, KNN, XGBoost for shape and size classification.
Step 11 : Evaluate models with: Accuracy, Precision, Recall, F1 Score, Confusion Matrix and ROC curve.
Step 12 : Stop

3 Results and Discussion

This experimentation was conducted to develop a unified pipeline integrating SAM-based segmentation with five machine learning classifiers for Ag-GO nanocomposite evaluation. The objective was to classify nanocomposites according to their size and shape,

thereby enhancing the accuracy and consistency of nanocomposites structural evaluation. In this study, SAM-based segmentation and machine learning classification, was evaluated on high-resolution SEM images of silver-graphene oxide (Ag-GO) nanocomposites. Figure 2 illustrates the sequential image processing and segmentation workflow. The original SEM image is shown in Fig. 2(a), which is subsequently pre-processed as presented in Fig. 2(b). The pre-processed image is then subjected to the segment anything model (SAM), resulting in a coloured mask image shown in Fig. 2(c). Finally, the individually segmented nanocomposites are displayed in Fig. 2(d), with each nanocomposite distinctly represented by a unique colour.

Segmentation of the SEM image resulted in the identification of 963 nanocomposites, which were further classified based on their structural morphology into three categories: elliptical, polygonal, and spherical shapes. Feature extraction included geometric properties (area, perimeter, aspect ratio, circularity, solidity, equivalent diameter). The resulting feature matrix was used for training five supervised classifiers. The implementation and analysis were carried out on Google Colab using Python notebooks with cloud-based GPU support.

A detailed morphological analysis of the segmented nanocomposite was performed to understand their structural distribution. Table 1 outlines the shape-wise morphological summary of Ag-GO nanocomposites. Elliptical nanocomposites exhibited moderate size and high solidity, indicating cohesive and uniform geometries. Polygonal nanocomposites, demonstrated lower circularity and solidity, reflecting irregular or angular structures. Spherical nanocomposites, although smaller in size, showed high circularity values. The shape of the nanocomposites provides an important insight into the nanoscale structure, which may influence the material's behaviour in biological or catalytic applications.

A total of 963 nanocomposites were analyzed from the SEM image dataset. The particles were grouped into five size categories: 0–50 nm, 51–100 nm, 101–150 nm, 151–200 nm, and above 200 nm. The distribution revealed that the majority of nanocomposites were in the 51–100 nm range, accounting for 410 nanocomposites (42.58). The 0–50 nm range was the second most prevalent, comprising 260 nanocomposites (27.00%). Nanocomposites in the 101–150 nm range represented 161 nanocomposites (16.72%), while those in the 151–200 nm category constituted 78 nanocomposites (8.10%). Only 54 nanocomposites (5.61%) were larger than 200 nm. Table 2 outlines the size-wise morphological summary of Ag–GO nanocomposites.

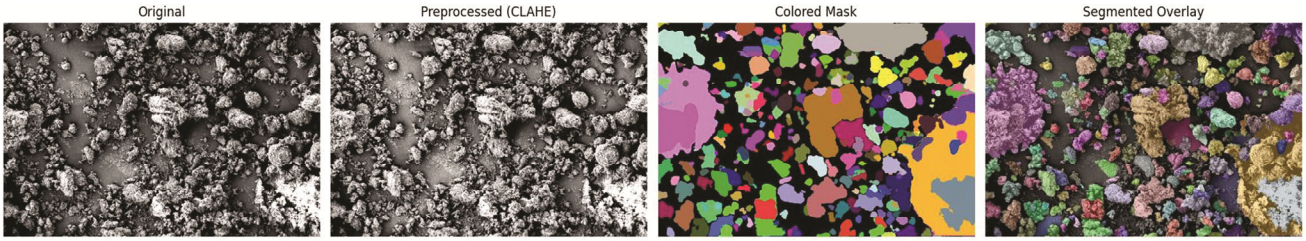

Fig. 2 — Sample SEM images of Ag-GO nanocomposites (a) Original image, (b) Pre-processed image, (c) Coloured mask image and (d) Segmented nanocomposite image.

Table 1 — Shape-wise morphological summary of Ag-GO nanocomposites.

Shape	Nanocomposites Count	Avg. Size (nm)	Avg. Perimeter (nm)	Avg. Circularity	Avg. Aspect Ratio	Avg. Solidity
Elliptical	553	93.72	360.47	0.692	1.670	0.898
Spherical	262	39.98	131.23	0.991	1.478	0.943
Polygonal	148	166.55	877.07	0.395	1.984	0.778

Table 2 —Size-wise morphological summary of Ag–GO nanocomposites.

Size Range	Elliptical	Polygonal	Spherical	Total	Percentage
0–50 nm	71	6	183	260	27.00%
51–100 nm	301	33	76	410	42.58%
101–150 nm	117	42	2	161	16.72%
151–200 nm	49	28	1	78	8.10%
201+ nm	15	39	0	54	5.61%
Total Nanocomposites	553	148	262	963	100.00%

This analysis demonstrates that the nanocomposite system is predominantly composed of nanocomposites below 100 nm, which together constitute nearly 70% of the total population. Such a size distribution is significant, as smaller nanocomposites generally exhibit a higher surface area–to–volume ratio, thereby enhancing their catalytic, optical, and electronic properties. The relatively low percentage of nanocomposites above 200+ nm suggests a narrow size distribution, indicative of good control during the synthesis process.

To automate the classification of nanocomposite shapes, we divided the dataset into two subsets: 80% for training the models and 20% for assessing their performance, and five supervised machine learning models were evaluated. Among the evaluated models, XGBoost demonstrated the highest classification accuracy of 97% on the test set, outperforming the other classifiers in terms of robustness and generalization capability. Table 3 shows the summary of the performance metrics of various machine learning models, including accuracy, precision, recall and F1-score. The high accuracy indicates the suitability of XGBoost in capturing complex, nonlinear patterns in the nanocomposite morphology data, making it a promising tool for automated structural characteristics analysis of nanocomposites.

The confusion matrices for shape classification are shown in Fig. 3. XGBoost achieved high accuracy across elliptical, polygonal, and spherical shapes,

Table 3 — Summary of performance metrics of various machine learning models.

Model	Morphology	Accuracy	Precision	Recall	F1-score
Random Forest	Shape	0.95	0.96	0.95	0.95
	Size	0.91	0.92	0.91	0.91
KNN	Shape	0.89	0.89	0.89	0.89
	Size	0.76	0.77	0.76	0.76
Logistic Regression	Shape	0.88	0.88	0.88	0.87
	Size	0.64	0.62	0.64	0.61
Decision Tree	Shape	0.92	0.92	0.92	0.92
	Size	0.90	0.90	0.90	0.90
XGBoost	Shape	0.97	0.97	0.97	0.97
	Size	0.95	0.95	0.95	0.95

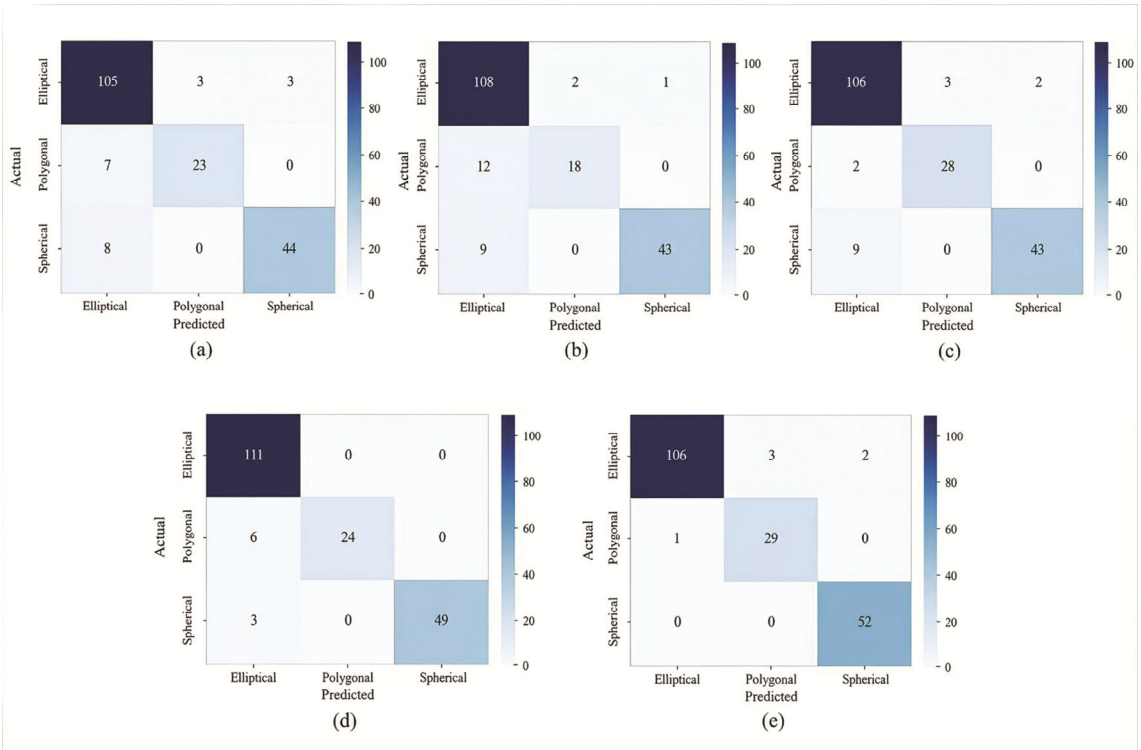

Fig. 3 — Confusion matrices for shape classification using (a) K-Nearest Neighbor (KNN), (b) Logistic Regression, (c) Decision Tree, (d) Random Forest and (e) XGBoost.

although minor misclassifications occurred between elliptical category. Logistic regression improved classification stability, particularly for spherical particles, while decision tree performance showed variability, with occasional misclassification of spherical as elliptical shapes. In contrast, ensemble models demonstrated superior discriminative ability. Random forest achieved near-perfect classification, with minimal overlap across categories.

The confusion matrices for size classification are presented in Fig. 4. KNN provided reasonable classification accuracy, but misclassification was more frequent for intermediate ranges (e.g., 101–150 nm and 151–200 nm), where size distributions overlap. Logistic regression improved results but still showed moderate confusion between 0–50 nm and 51–100 nm classes. Decision tree classifiers performed well for the smallest (0–50 nm) and mid-size ranges (101–150 nm), though they were less reliable for the 151–200 nm group. Random forest and XGBoost again outperformed simpler models. Both achieved highly accurate classification across all five size categories, with minimal misclassifications.

Model performance for nanocomposite size and shape classification was assessed using ROC curves and AUC values. XGBoost further enhanced performance, showing almost complete agreement between predicted and actual classes for all three shapes. These results are consistent with the ROC-AUC analysis as shown in Fig. 5, confirming that ensemble models are highly effective in separating nanocomposites shapes with overlapping morphological features.

For size classification, KNN and logistic regression achieved good discrimination with AUC values ranging from 0.81 to 0.95, although performance was inconsistent across intermediate size ranges. Decision tree models performed well for smaller size categories but showed reduced accuracy for particles in the 151–200 nm range (AUC = 0.77). In contrast, Random Forest and XGBoost models provided superior performance, achieving near-perfect separation across all size classes (AUC = 0.99–1.00). ROC curves of shape classification using different machine learning models is as shown in Fig. 6.

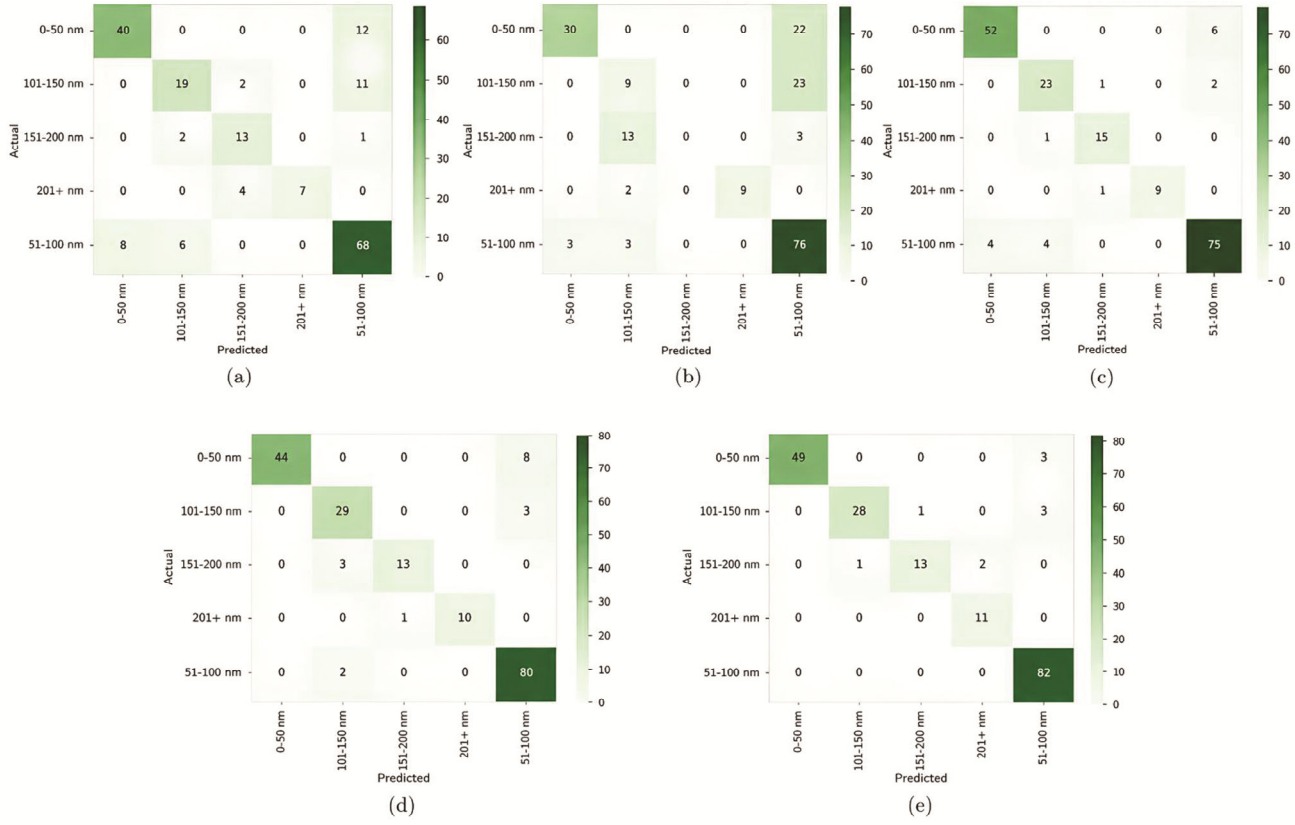

Fig. 4 — Confusion matrices for size classification using (a) K-Nearest Neighbour (KNN), (b) Logistic Regression, (c) Decision Tree, (d) Random Forest and (e) XGBoost.

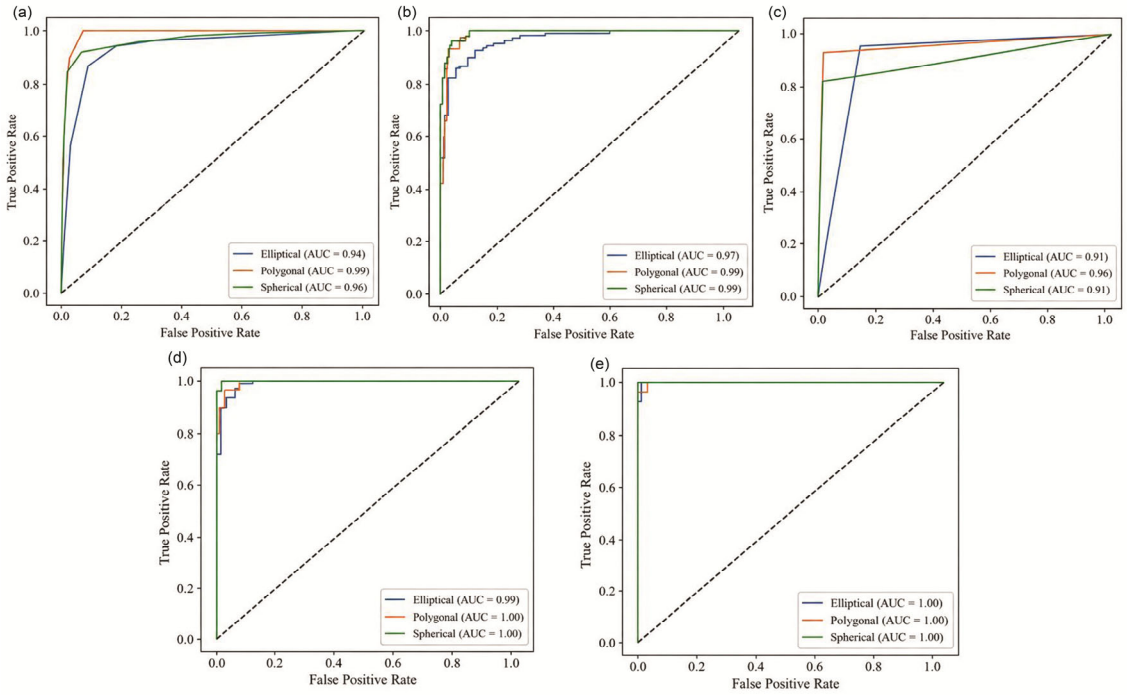

Fig. 5—ROC curves of size classification using (a) K-Nearest Neighbor (KNN), (b) Logistic Regression, (c) Decision Tree, (d) Random Forest and (e) XGBoost.

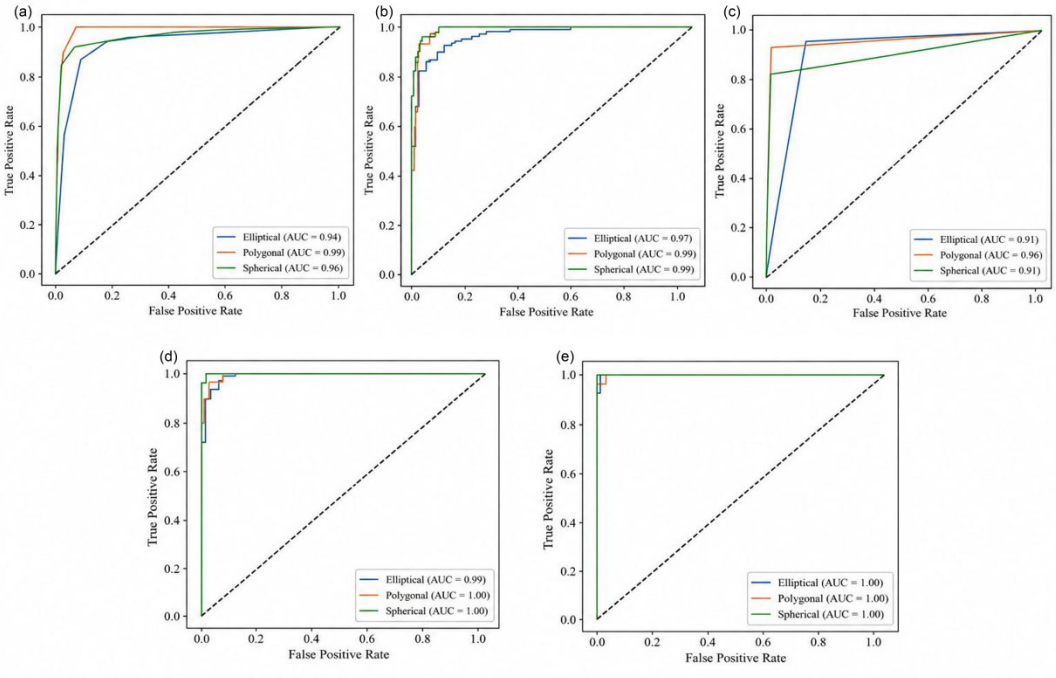

Fig.6 —ROC curves of shape classification using (a) K-Nearest Neighbor (KNN), (b) Logistic Regression, (c) Decision Tree, (d) Random Forest and (e) XGBoost.

4 Conclusion

The present study develops a structured workflow for the segmentation and classification of silver-graphene oxide nanocomposites from SEM images. The use of the segment anything model (SAM) enabled precise segmentation of individual

nanocomposites, and the subsequent extraction of geometric features such as size and shape have provided an effective basis for classification. Among the five machine learning models evaluated, XGBoost achieved the highest performance, with 97% accuracy for shape classification, 95% accuracy for size classification, and an AUC close to 1. Random Forest and KNN also exhibited strong results, supporting the effectiveness of ensemble-based methods in handling complex feature analysis. The proposed framework is generalizable and can be extended to other nanomaterials and microscopy image datasets. In the future, we plan to study the structural characteristics of different metal oxide nanocomposites using deep learning models.

Acknowledgement

The authors are grateful to the Department of Chemistry and the Department of Computer Science, Rani Channamma University, Belagavi, for providing the experimental and computational facilities required to carry out this research work.

References

1 Kahraman O, Turunc E & Binzet R, *Microchemical Jl*, 206 (2024) 111587.
2 Nam N T H, Dat N M, Hai N D, Huong L M, Tai L T & Dat N T, *New J Chem*, 47 (2023) 8090.
3 Thinh D B, Dat N M, Tuyen N N K, Tai L T, Hai N D & Tinh N T, *Vietnam J Chem*, 60 (2022) 553.
4 Malik S B, Saggu J I, Gul A, Abbasi B A, Iqbal J & Waris S, *Molecules*, 27 (2022) 5184.
5 Jamjoum H A A, Umar K, Adnan R, Razali M R & Ibrahim M N M, *Frontiers Chem*, 9 (2021) 752276.
6 Kumari S, Sharma P, Yadav S, Kumar J, Vij A & Rawat P, *ACS Omega*, 5 (2020) 5041.
7 Gurubasavaraj P M, Anigol L B & Sajjan V P, *Indian J Sci Technol*, 16 (2023) 1777.
8 Li C, Wang X, Chen F, Zhang C, Zhi X, Wang K & Cui D, Biomaterials, 34 (2013) 3882.
9 Das T K, Ghosh S K & Das N C, *Nano-Structures & Nano-Objects*, 34 (2023) 100960
10 Ji Z & Wang Y, Journal of Nanomaterials, 2022 (2022) 4964368.
11 Yang L, Wang H, Leng D, Fang S, Yang Y & Du Y, Chem Eng J, 500 (2024) 156687.
12 Abebe W, Strube J, Guo L, Tallent N R, Bel O, Spurgeon S, Doty C & Jannesari A, *Comput Mater Sci*, 246 (2025) 113400.
13 Monteiro G A, Monteiro B A, Dos Santos J A & Wittemann A, *Scientific Reports*, 15 (2025) 2341.
14 Gaines T B, Boyle C, Keller J M, Maschmann M R, Price S & Scott G J, Proceedings of the IEEE Conference on Artificial Intelligence,IEEE (New York), 2024, pp. 1266.
15 Lu S, Montz B, Emrick T & Jayaraman A, *Digital Discovery*, 1 (2022) 816.
16 Papia E-M, Kondi A & Constantoudis V, *Microporous Mesoporous Mater.*, 394 (2025) 113675.
17 Bannigidad P, Potraj N & Gurubasavaraj P M, Indian Journal of Science and Technology, 16 (2023) 1284.
18 Jahanian M, Hosseini S S, Azimian Dehkordi Z, Sadeghi K, Rostam Niakan Kalhori S, Ayyoubzadeh S M & Ahmadi M,Mater Today Commun, 41 (2024) 110818.
19 Xu Y, Xu D, Yu N, Liang B, Yang Z & Asif M S, ACS Applied Materials & Interfaces, 15 (2023) 18244.
20 Prasad A, Santra T S & Jayaganthan R, Metals, 14 (2024) 539.
21 Tao H, Wu T, Aldeghi M, Wu T C, Aspuru-Guzik A & Kumacheva E, *Nature Reviews Materials*, 6 (2021) 701.
22 Saxena A, Polin N, Kusampudi N, Katnagallu S, Molina-Luna L, Gutfleisch O, Berkels B, Gault B, Neugebauer J & Freysoldt C, MicroscMicroanal, 29(5) (2023) 1658.
23 Zhong X, Liang G, Meng L, Xi W, Gu L, Tian N, Zhai Y *et al*., *Nanomaterials*, 15 (2025) 1886.
24 Shah A, Schiller J A, Ramos I, Serrano J, Adams D K, Tawfick S & Ertekin E, Mater Today Commun, 35 (2023) 106127.
25 Araujo E S, Pereira M F, da Silva G M, Tavares G F, Oliveira C Y & Faia P M, Toxics, 11 (2023) 658.
26 Xie M, Gao M, Yun Y, Malmsten M, Rotello V M & Zboril R, Angewandte Chemie International Edition, 62 (2023) e202217345.
27 Lange A, Sawosz E, Wierzbicki M, Kutwin M, Daniluk K, Strojny B & Jaworski S, Materials, 15 (2022) 3122.
28 Singh J P, Nandi T & Ghosh S K, Applied Surface Science, 542 (2021) 148410.
29 Yu R, Zhu C, Wan J, Li Y & Hong X, Polymers, 13 (2021) 151.
30 Bannigidad P, Potraj N & Gurubasavaraj P, *5th EAI International Conference on Big Data Innovation for Sustainable Cognitive Computing*, (Springer Cham, Switzerland), ISBN: 978-3-031-28323-9, 2023, pp. 27–38.
31 Negi P, Chadha J, Harjai K, Gondil V S, Kumari S & Raj K, Biomedicines, 12 (2024) 1104.